Examining Geometric Integration for Propagating Orbit Trajectories with Non-Conservative Forcing

Course Project for CDS 205 - Geometric Mechanics

John M. Carson III
California Institute of Technology

June 1, 2005

Abstract

The precision of numerical integration greatly affects the ability to track and navigate a spacecraft throughout the solar system. In fact, precision of up to fifteen significant digits is required for accurate navigation of spacecraft missions heading toward the outer planets. This paper explores the use of numerical integration techniques based symplectic and variational integrators to propagate orbit trajectories, plus an examination is made of how to incorporate into these methods the non-conservative forces affecting the trajectories. These numerical techniques are of interest due to their intrinsic ability to conserve quantites such as energy, momentum, the Hamiltonian, etc. from the inherent dynamics.

Research Objective

The ability to successfully navigate the solar system is directly related to how well a spacecraft state can be predicted. State determination is accomplished through both estimation from Earth-based observations, as well as through numeric propagation of governing equations of motion. Traditional techniques for numerical integration are RK (Runge-Kutta) and similar advanced discretization techniques that typically require small step sizes to ensure precision in the trajectory propagation of large solar distances. A benefit of these techniques is in their ability to incorporate non-conservative forces, along with starts and stops of the propagation in order to include different perturbations. The objective of this research is to implement symplectic and variational integrators for propagating orbit trajectories and to determine the feasibility and methodology for incorporating non-conservative forces and perturbations into the developed techniques.

The approach to this research will be a step-wise increase in complexity of the orbit problem. The first step will be to formulate the Hamiltonian for a simple two-body problem (involving a spacecraft in the gravity well of a single planet) with no external forcing other than the gravitational potential of the host planet (See simple schematic in figure 1). In addition, the integration scheme for a basic symplectic integrator will be developed and formulated for this initial problem; the chosen symplectic integrator will be based on the midpoint rule. This first step will facilitate comparisons with classic RK methods (such as variable and fixed time step methods) since the two-body problem has analytic solutions. Further, this step will enable an assessment of step size on numerical accuracy.

The second stage of this research will demonstrate that the chosen midpoint rule is not only a symplectic integrator but also a variational integrator. Through this extension, which comes

through the discrete Euler-Lagrange equations (DEL) and the discrete Legendre transform, a possible method of incorporating non-conservative forces becomes apparant. The third stage of the research will consider how non-conservative forcings enter variational integration schemes through the use of the d'Alembert Principle. Either the DEL-like approach just mentioned will be considered, or perhaps a return to the Hamiltonian-side of mechanics will be necessary.

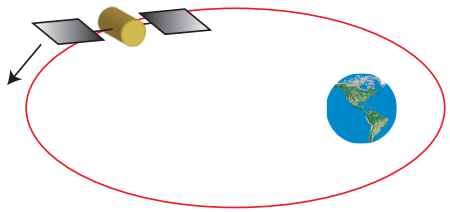

Figure 1: Representation of Two-Body Problem

The second step of the research will introduce impulsive forces at preset times in order to determine how symplectic versus RK propagation handles the change in trajectory direction. Again, the analytic solutions for two-body orbit mechanics are known, so meaningful comparisons can be made. To implement the impulsive forces, both integrators will be stopped, and a step change in velocity will be made to current velocity values (thus imparting an impulsive force). The impulsive force is essentially bumping the energy (Hamiltonian) of the orbit to a new, constant level.

The third step of the research will be to determine how to incorporate non-conservative forces into the equations of motion such that symplectic integration remains valid. The technique for doing this is not yet known, however, there are known classes of systems that conserve a Hamiltonian but not energy. Further, the notion of being locally Hamiltonian may play an important role in this implementation. This all remains to be determined through the research.

Equations of Motion

The dynamics of an orbiting spacecraft under the influence of only gravity obey a conservation of energy principal from which the equations of motion can be derived [1]. The energy (and Hamiltonian) for a spacecraft orbiting a planet is given by

$$H(\mathbf{q},\mathbf{p}) = \frac{1}{2m}||\mathbf{p}||^2 - \frac{m\mu}{q} \tag{1}$$

where $q = ||\mathbf{q}||$ is the radius from the planet c.m. (center of mass), m is the spacecraft mass, μ is the gravitational parameter for a particular planets or body being orbited, and $\mathbf{p}$ is the spacecraft momentum. The spacecraft mass is assumed insignificant to the planet mass, so the spacecraft exerts no influence on the planet's orbit. Thus, the center of gravity of the two-body system remains fixed at the planet c.m.

The Hamiltonian in equation 1 governs the resulting equations of motion:

$$\left.\begin{array}{l} \frac{\partial \mathbf{q}}{\partial t} = \frac{\partial H}{\partial \mathbf{p}} = \frac{1}{m}\mathbf{p} \\ \\ \frac{\partial \mathbf{p}}{\partial t} = -\frac{\partial H}{\partial \mathbf{q}} = -\frac{m\mu}{q^3}\mathbf{q} \end{array}\right\} \quad \dot{\mathbf{z}} = \mathbb{J}\nabla H(\mathbf{z}) \tag{2}$$

where $\mathbf{z} = (q,p)^T$ and $\mathbb{J} = \begin{bmatrix} 0 & I \\ -I & 0 \end{bmatrix}$. Note also the second-order equation of motion that arises from the left hand side of equation 2: $m\ddot{\mathbf{q}} = -\frac{m\mu}{q^3}\mathbf{q}$.

For spacecraft orbiting multi-body systems (i.e.. systems with one spacecraft and multiple planets), a conservation of energy principal exists as well. However, the presence of non-conservative forces causes energy not to be conserved.

Symplectic Integration

For a $2n$-dimensional symplectic vector space (Z, Ω), let $z = (q, p) \in Z$ denote canonical coordinates such that symplectic matrix $\mathbb{J}$ represents Ω. The evolution equations of a Hamiltonian system on phase space Z are given by

$$\dot{z} = \mathbb{J}\nabla H(z), \quad \text{with } z|_{t=0} = z_0$$

where $\mathbb{J} = \begin{bmatrix} 0 & I \\ -I & 0 \end{bmatrix}$.

Proposition 1. *The mapping $\phi : z_n \in Z \to z_{n+1} \in Z$ based on the midpoint rule*

$$\dot{z} = \frac{z_{n+1} - z_n}{\Delta t} \qquad z = \frac{z_{n+1} + z_n}{2}$$

is symplectic, such that

$$z_{n+1} = z_n + \Delta t \mathbb{J}\nabla H\left(\frac{z_{n+1} + z_n}{2}\right) \tag{3}$$

Proof. For this mapping to be symplectic, the Jacobian of the update scheme must be symplectic:

$$\begin{aligned} \frac{\partial z_{n+1}}{\partial z_n} &= I + \Delta t \mathbb{J} \frac{\partial}{\partial z_n} \nabla H\left(\frac{z_{n+1} + z_n}{2}\right) \\ &= I + \frac{1}{2}\Delta t \mathbb{J}\nabla^2 H\left(\frac{z_{n+1} + z_n}{2}\right)\left(I + \frac{\partial z_{n+1}}{\partial z_n}\right) \end{aligned} \tag{4}$$

From equation 4, define the following:

$$A = \frac{1}{2}\Delta t \mathbb{J}\nabla^2 H \tag{5}$$

where $\nabla^2 H$ is evaluated at $\left(\frac{z_{n+1}+z_n}{2}\right)$. Then, equation 4 can be re-written as

$$\begin{aligned} (I - A)\frac{\partial z_{n+1}}{\partial z_n} &= I + A \\ \frac{\partial z_{n+1}}{\partial z_n} &= (I - A)^{-1}(I + A) \end{aligned} \tag{6}$$

where an assumption has been made on the invertibility of $I - A$. In other words, the Hessian of H and the size of Δt are such that $I - A$ is invertible.

Assuming provided $I - A$ is invertible, the right-hand side of equation 6 is the Cayley transform, which is symplectic if and only if A is Hamiltonian [2, p. 80]. Since A is a linear mapping, then A is Hamiltonian if and only if A is Ω-skew [2, Prop. 2.5.1, p. 77]. And, Ω-skewness of A is equivalent to the matrix $\mathbb{J}A$ being symmetric (i.e.. $\mathbb{J}A + A^T\mathbb{J} = 0$) [2, p. 78]. Thus, evaluate A from equation 5 as follows:

$$\begin{aligned}\mathbb{J}A + A^T\mathbb{J} &= \mathbb{J}\left(\frac{1}{2}\Delta t\mathbb{J}\nabla^2 H\right) + \left(\frac{1}{2}\Delta t\mathbb{J}\nabla^2 H\right)^T\mathbb{J} \\ &= \frac{1}{2}\Delta t\left(\mathbb{J}\mathbb{J}\nabla^2 H + \left(\nabla^2 H\right)^T\mathbb{J}^T\mathbb{J}\right) = \frac{1}{2}\Delta t\left(-I\cdot\nabla^2 H + \nabla^2 H\cdot I\right) \\ &= 0\end{aligned}$$

since $\nabla^2 H$ is symmetric. Thus, A is Ω-skew, implying A is Hamiltonian. Finally, by the Cayley transform, equation 6 is symplectic, indicating equation 3 defines a symplectic mapping. $\square$

Implementing Symplectic Integration

The difficultly with implementing the symplectic integration scheme of equation 3 is that the method is implicit. An initial method for dealing with this problem is to utilize a Newton solve for finding the roots of the equation. Equation 3 can be viewed as

$$f(z_{n+1}) = z_{n+1} - z_n - \Delta t\mathbb{J}\nabla H\left(\frac{z_{n+1}+z_n}{2}\right) = 0 \tag{7}$$

where the roots of function f are the solutions z_{n+1} to equation 3. The Newton solve is initiated with a guess, such as guess $= z_n$, such that

$$f(z_{n+1}) = 0 = f(\text{guess} + \delta) \approx f(\text{guess}) + f'(\text{guess})\delta \tag{8}$$

with $f'(\text{guess})$ being the Jacobian of f, as given in equation 6. The value of δ is determined from equation 8:

$$\delta = -(f'(\text{guess}))^{-1} f(\text{guess})$$

which is used to iterate on the initial guess (guess $=$ guess $+ \delta$) until $f(\text{guess}) < \epsilon$ for some desired, small value of ϵ.

Variational Algorithms and Variational Integration [3]

The action integral on a Lagrangian $L(q, \dot{q})$ is defined as

$$S = \int_a^b L(q(t), \dot{q}(t))dt \tag{9}$$

where the Euler-Lagrange equations extremize S given fixed end points. The development of a discrete version of the Euler-Lagrange equations involves discretizing the action integral S over a time step Δt such that

$$L_d(q_k, q_{k+1}) = \int_{t_k}^{t_{k+1}} L(q(t), \dot{q}(t))dt \approx L(\tilde{q}, \dot{\tilde{q}})\Delta t \tag{10}$$

where $L(\tilde{q}, \dot{\tilde{q}})$ is constant over the interval $t \in (t_k, t_{k+1})$ with $\tilde{q}$ and $\dot{\tilde{q}}$ a discrete approximation for q and $\dot{q}$ and $t_{k+1} - t_k = \Delta t$. This defines a discrete Lagrangian such that $L_d : Q \times Q \to \mathbb{R}$. The associated discrete analog to the action integral is then given by

$$S_d = \sum_{k=0}^{N-1} L_d(q_k, q_{k+1}), \tag{11}$$

where $S_d : Q^{N+1} \to \mathbb{R}$, and similar to the continuous case, extremizing S_d produces the discrete version of the Euler-Lagrange equations or DEL (Discrete Euler-Lagrange) equations:

$$D_1 L_d(q_{k+1}, q_{k+2}) + D_2 L_d(q_k, q_{k+1}) = 0 \tag{12}$$

for $k = 1, ..., N-1$. Note, equation 12 defines a variational algorithm.

The Legendre transform has an analogous discrete version, as defined in [3],

$$\mathbb{F}L_d : Q \times Q \to T^*Q; (q_k, q_{k+1}) \mapsto (q_{k+1}, D_2 L_d(q_k, q_{k+1})) \tag{13}$$

which further implies $p_{k+1} = D_2 L_d(q_k, q_{k+1})$.

For the research conducted herein, the discrete approximation to the continuous Lagrangian is chosen to be the symmetric form

$$\begin{aligned} L_d^{sym,\alpha}(q_k, q_{k+1}) = &\frac{\Delta t}{2} L\left((1-\alpha)q_k + \alpha q_{k+1}, \frac{q_{k+1} - q_k}{\Delta t}\right) \\ &+ \frac{\Delta t}{2} L\left(\alpha q_k + (1-\alpha) q_{k+1}, \frac{q_{k+1} - q_k}{\Delta t}\right) \end{aligned} \tag{14}$$

Theorem 1. *[3] The midpoint rule in equation 3 is a variational algorithm through the discrete Legendre tranformation with the discrete Lagrangian $L_d^{sym,\alpha}$ for $\alpha = \frac{1}{2}$.*

Proof. (*in the reverse direction*)
Let $q_m = \frac{q_{k+1}+q_k}{2}$ and $\dot{q} = \frac{q_{k+1}-q_k}{\Delta t}$, then for $\alpha = \frac{1}{2}$,

$$L_d^{sym,\frac{1}{2}}(q_k, q_{k+1}) = \Delta t \; L\left(\frac{q_k + q_{k+1}}{2}, \frac{q_{k+1} - q_k}{\Delta t}\right) = \Delta t \; L(q_m, \dot{q}_m) \tag{15}$$

and

$$D_1 L_d^{sym,\frac{1}{2}}(q_k, q_{k+1}) = \frac{\Delta t}{2} D_1 L(q_m, \dot{q}_m) - D_2 L(q_m, \dot{q}_m) \tag{16}$$

$$D_2 L_d^{sym,\frac{1}{2}}(q_k, q_{k+1}) = \frac{\Delta t}{2} D_1 L(q_m, \dot{q}_m) + D_2 L(q_m, \dot{q}_m) \tag{17}$$

Through the DLT (discrete Legendre transform) in equation 13 and the DEL equations (equation 12),

$$p_k \overset{DLT}{\underset{\downarrow}{=}} D_2 L_d(q_{k-1}, q_k) \overset{DEL}{\underset{\downarrow}{=}} -D_1 L_d(q_k, q_{k+1}) \tag{18}$$

$$p_{k+1} = D_2 L_d(q_k, q_{k+1}) \tag{19}$$

which defines an implicit algorithm such that $(q_k, p_k) \mapsto (q_{k+1}, p_{k+1})$. For $L_d^{sym,\frac{1}{2}}$, the variables p_k and p_{k+1} are equivalent to equations 16 and 17, respectively.

Adding and subtracting equations 18 and 19, plus incorporating the results of equations 16 and 17 for $\alpha = \frac{1}{2}$ provides the following algorithms:

$$\frac{p_{k+1} - p_k}{\Delta t} = D_l L(q_m, \dot{q}_m) \tag{20}$$

$$\frac{p_{k+1} + p_k}{2} = D_2 L(q_m, \dot{q}_m) \tag{21}$$

Restrict the class of Lagrangian to those of canonical form

$$L(q, \dot{q}) = \frac{1}{2} \dot{q}^T M \dot{q} - V(q) \tag{22}$$

where M is a symmetric matrix, and V is a potential function. Note, this loses the generality in the proof, but this class of Lagrangian is valid for most mechanical systems, including those in the research within this paper. The continuous Legendre transform provides the following Hamiltonian for this class of canonical system:

$$H(q,p) = p^T\dot{q} - L(q,\dot{q}) = \frac{1}{2}M^{-1}p^Tp + V(q) \tag{23}$$

with $p = M\dot{q}$

For the Lagrangian of equation 22, the first and second slot derivatives are

$$D_1L(q,\dot{q}) = -\nabla V(q) \qquad \text{and} \qquad D_2L(q,\dot{q}) = M\dot{q} \tag{24}$$

which when combined with the algorithms in equations 20 and 21 result in the following equations

$$\frac{p_{k+1}-p_k}{\Delta t} = -\nabla V(q_m) = -\nabla V(\frac{q_{k+1}+q_k}{2}) \quad \Rightarrow \quad \frac{p_{k+1}-p_k}{\Delta t} = -\frac{\partial H}{\partial q}\left(\frac{q_{k+1}+q_k}{2}\right) \tag{25}$$

$$\frac{p_{k+1}+p_k}{2} = M\dot{q}_m = M\frac{q_{k+1}-q_k}{\Delta t} \quad \Rightarrow \quad \frac{q_{k+1}-q_k}{\Delta t} = \frac{\partial H}{\partial q}\left(\frac{p_{k+1}+p_k}{2}\right) \tag{26}$$

which are the exactly the form of equation 3 for $z = (q,p)$ and the Hamiltonian of equation 23. Thus, the midpoint rule defines a variational algorithm with $L_d^{sym,\alpha}$ when $\alpha = \frac{1}{2}$. □

Incorporating Non-Conservative Forces

The results of Theorem 1 are quite powerful and provide a framework from which non-conservative forces might be incorporated into variational-like algorithms. No results will be shown from this brief section but it serves as a basis for how future work will continue. As discussed in [3], the integral Lagrange-d'Alembert principal is given by

$$\delta\int L(q(t),\dot{q}(t))dt + \int F(q(t),\dot{q}(t))dt = 0 \tag{27}$$

which appears similar to the action integral in equation 9. In fact, a discrete version of equation 27 exists from which forced DEL equations can be derived:

$$D_1L_d(q_{k+1},q_{k+2}) + D_2L_d(q_k,q_{k+1}) + F_d^-(q_{k+1},q_{k+2}) + F_d^+(q_k,q_{k+1}) = 0 \tag{28}$$

From these forced DEL equations, an implicit algorithm is likely derivable in a manner analogous to that from the proof of Theorem 1. A key to the development of this algorithm will require appropriate discretization of the non-conservative forces, likely in a symmetric fashion as with $L_d^{sym,\alpha}$.

Application of Symplectic/Variational Integration to Circular Orbits

The first-order symplectic integration scheme from equation 3 was implemented in Matlab for the Hamiltonian dynamics of equation 1 for a spacecraft orbiting a planet (two orbit types are analyzed, one circular and one elliptic). The parameters chosen for the spacecraft and planet are given in table 1. Consequently, the initial conditions also set the value of the conserved Hamiltonian from equation 1 for the two orbit types; the Hamiltonian values for each orbit type are included in the table (they are negative, which corresponds to circular and elliptic orbits).

Table 1: Simulation Parameter Data and Initial Conditions

μ (km^3/s^2)	3200.9998
m (kg)	1
$\mathbf{q}_0$ (km)	$(0, 1664.029, 0)^T$
$\mathbf{p}_0(circular)$ (km/s)	$(1.386955, 0, 0)^T$
$H(q,p)(circular)$ (kg·km^2/s^2)	-0.96182211
$\mathbf{p}_0(elliptic)$ (km/s)	$(1.550663, 0, 0)^T$
$H(q,p)(elliptic)$ (kg·km^2/s^2)	-0.72136658

The Matlab code also implements three additional schemes for comparing numerical performance over roughly one day (86400 seconds) of orbit data. The comparison schemes were the Matlab intrinsic RK45 scheme ODE45 (which has a variable time step) and two Mathworks fixed-step RK schemes called ODE2 and ODE4 (RK2 and RK4, respectively), available from the company web site.

Two orbit types were simulated with the numerical integrators: a circular orbit and an elliptical orbit. With both simulations, which are two-body conic orbits, analytic solutions for the orbits are available, which facilitates comparison of numerical schemes and determination of their accuracy.

Circular Orbit Simulation

Figure 2 juxtaposes results from the symplectic, RK45, and RK4 integration schemes, along with an analytic solution for the two-body circular orbit. Due to the choice of initial conditions, the orbit is planar.

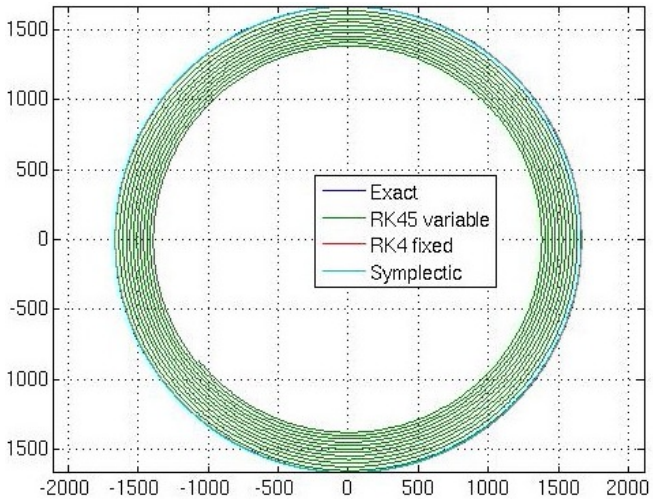

Figure 2: Comparison of Numerical Techniques Versus the Analytic Solution

From figure 2, the variable-step RK45 scheme is seen to wind toward the planet; the method is essentially dissipating energy from the orbit trajectory. The symplectic and RK4 (fixed-step) schemes track the exact orbit more closely and cannot be separated in figure 2. To distinguish these two schemes, figure 3 zooms in on a segment in the upper-left portion of figure 2.

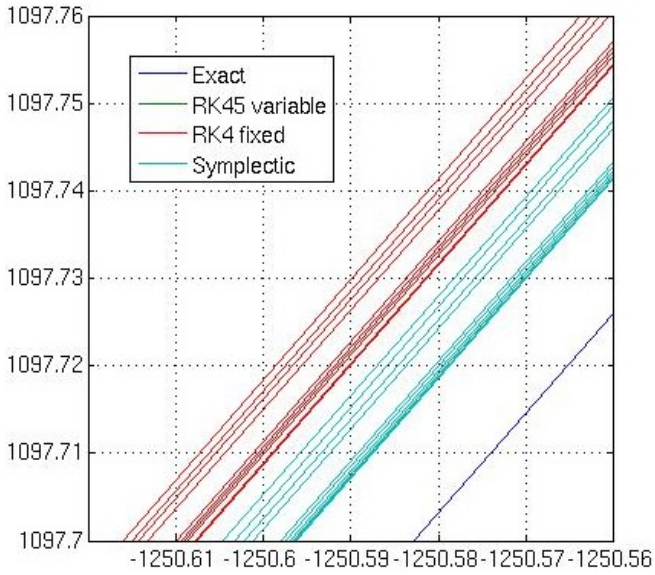

Figure 3: Close-Up of Circular Orbit from Figure 2

The close up of figure 3 reveals that both the RK4 and symplectic integrators track the analytic solution well, though both with an offset. Interestingly the symplectic integrator has a smaller offset than the RK4 method, which is interesting given that RK4 is fourth order and this particular symplectic scheme is second order. Utilizing an integrator that intrinsically accounts for the system geometry (conserving the Hamiltonian) does have benefit over a more naive technique, at least with a simple circular orbit. The conservation of energy by the symplectic integrator is revealed in figure 4, which also clearly shows how RK4 introduces false dissipation, something that would cause a loss in accuracy over long-term integration. The dissipation is in the 10^{th} digit only during this time interval, so the plot scale is cryptic.

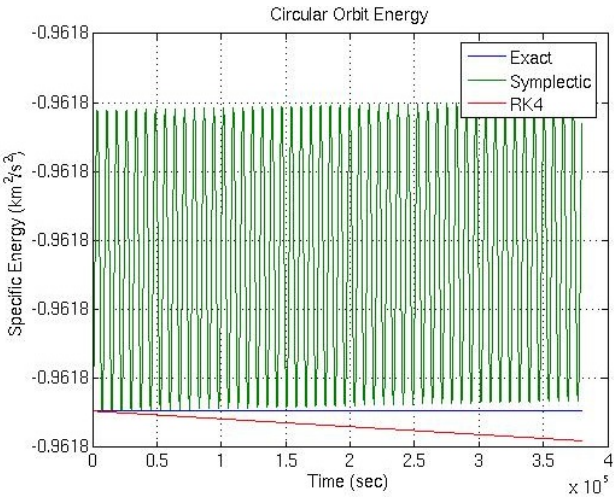

Figure 4: Energy of Circular Orbit should be Conserved

Elliptical Orbit Simulation

Figure 5 juxtaposes results from all four integration schemes (symplectic, RK2, RK4, and RK45), along with an analytic solution for the two-body elliptic orbit. The orbit is again planar due to the choice of initial conditions; for the elliptic.

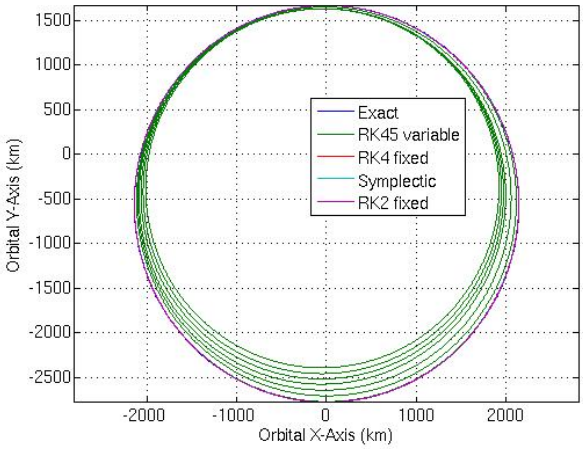

Figure 5: Comparison of Numerical Techniques Versus the Analytic Solution

From figure 5, the variable-step RK45 scheme is again seen to wind toward the planet, artificially dissipating energy as was the case with the circular orbit. The remaining schemes track the exact orbit more closely, which can be seen in the zoom of the orbit shown in figure 6.

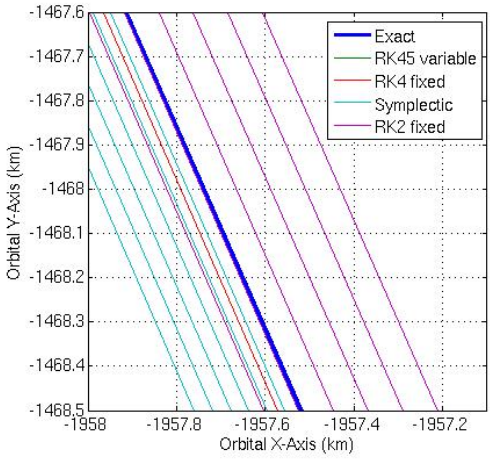

Figure 6: Close-Up of Ellipse Orbit from Figure 5

The close up of figure 6 shows that the RK4 integrator is significantly more accurate than the symplectic or RK2 technique. This is slightly differing from the circular case but seems reasonable since the RK4 technique is 4th-order, whereas the RK2 and chosen symplectic techniques are both second order. Outside of the circular case, these plots would appear to make the RK4

technique the integrator of choice. However, an examination of the energy of the system brings additional understanding of the ability of the different schemes to produce longterm accuracy (See figures 7 and 8).

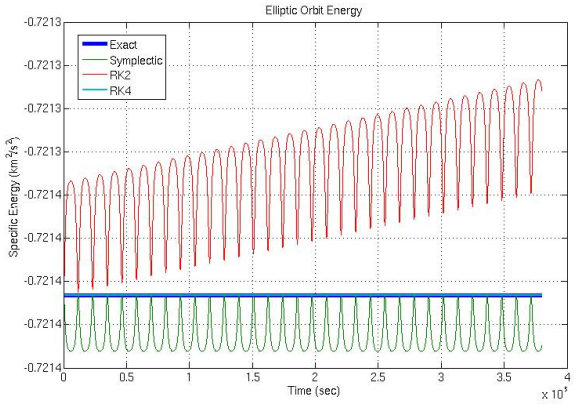

Figure 7: Elliptic Orbit Energy Showing RK2 Decay and Symplectic Conservation

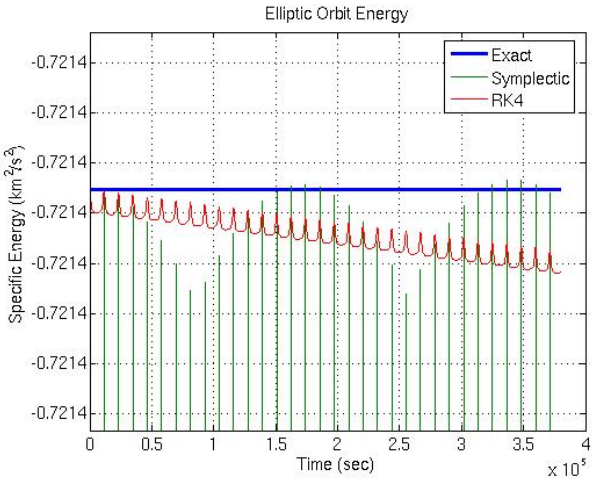

Figure 8: Close-Up of Elliptic Orbit Energy Revealing Slow Decay in RK4

The results of figures 7 and 8 indicate that the symplectic integrator, though not constant in energy, oscillates about a mean value, offset from the actual energy. A correction factor is likely realizable for the numerical implementation of the symplectic integrator that would make it oscillate about the exact value. The RK4 technique appears to conserve energy too in figure 7; however, a closer examination in figure 8 again shows that a very long-term integration would exhibit energy decay with RK4. Note, the number of significant digits displayed in the MATLAB generated plots is cryptic as it does not reflect the dissipation occurring in the 10th digit for the RK4 energy, though the trend in the plot is unmistakable.

Future Steps

One immediate question to answer is how versatile is the symplectic/variational integrator approach? The RK methods and other similar techniques can incorporate discretization of non-conservative forces and produce certain known accuracies. However, can the forced DEL equations produce their own variational-like algorithms that preserve some element of the forced dynamics, thus providing an even higher accuracy than traditional techniques? This question is of immediate interest to the research in this paper.

The subsequent focus of this research will be to incorporate non-conservative forces, such as thruster firings and solar radiation pressure. From the addition of these forces, performance and precision comparisons can be made with existing integration techniques. To assess precision and accuracy, simple two-body orbits with impulsive thruster firings can be propagated to determine how well different numerical integration schemes track the known, analytic solutions.

For an integration scheme to be useful in the real-world spacecraft navigation, the scheme must have high precision and have timely performance. Future work can focus on the integration scheme itself; the midpoint rule is the lowest-order symplectic integrator, so higher-order schemes should be more accurate. Accuracy requires not only reproducing proper position and velocity solutions but also arriving at the solutions on a similar time scale; for instance, the period of a conic orbit should be recoverable from the integration scheme. Regarding performance, explicit formulations, or good approximations to implicit forms could likely improve performance, so such ideas will be explored.

References

[1] R.R. Bate, D.D. Mueller, and J.E. White, *Fundamentals of Astrodynamics*, Dover Publications, 1971.

[2] J.E. Marsden and T.S. Ratiu, *Introduction to Mechanics and Symmetry*, Springer, 2^{nd} edition, 2002.

[3] C. Kane, J.E. Marsden, M. Ortiz, and M. West, *Variational Integrators and the Newmark Algorithm for Conservative and Dissipative Mechanical Systems*, Int. J. Num. Math. Eng., 49, pp. 1295-1325, 2000.